Cell Biochem Biophys (2016) 74:19–27
DOI 10.1007/s12013-015-0705-6

ORIGINAL PAPER

Polystyrene Nanoparticles Activate Erythrocyte Aggregation and Adhesion to Endothelial Cells

Gregory Barshtein[1] · Leonid Livshits[2] · Leonid D. Shvartsman[3] · Noa Ofek Shlomai[4] · Saul Yedgar[1] · Dan Arbell[5]

Published online: 31 July 2015

Abstract Nanoparticles (NPs) are drawing an increasing clinical interest because of their potential use as drug carriers. Recently, a new strategy for elevation of NPs in vivo circulation time has been proposed, specifically, utilizing red blood cells (RBCs) as a carrier for NPs, that are loaded with a drug, by interaction (in vitro) of human RBCs with NPs (RBC_{NP}). This class of delivery set-up, combines advantages of natural RBCs and synthetic biomaterials. Previous studies demonstrated that NPs initiated hemolysis of RBC and activated cells aggregation. In the present study, we examined the effect of RBC_{NP} on the aggregation of RBC and their adhesion to endothelial cells (EC). Red cells were treated with polystyrene NPs (PS-NP), and following their washing, were added to suspension of untreated cells at various concentrations. We observed that the PS-NP and RBC_{NP} initiated the formation of red cells aggregates and markedly elevated RBC adhesion to EC. These effects were augmented with (a) increasing concentration of NPs or RBC_{NP}, and (b) with decreasing NP size. This implies that RBC_{NP} are cells with a stronger intercellular interaction, and may thereby induce the formation of large and strong aggregates with untreated RBC, as well as strong RBC/EC interaction.

Keywords Nanoparticles · Hemolysis · Erythrocyte adhesion · Erythrocytes aggregation

✉ Saul Yedgar
yedgar@md.huji.ac.il

1 Department of Biochemistry, The Faculty of Medicine, Hadassah Medical School, The Hebrew University, 91120 Jerusalem, Israel

2 The Diabetes Research Center, Hadassah Hebrew University Medical Center, Jerusalem, Israel

3 The Racah Institute of Physics, The Hebrew University, Jerusalem, Israel

4 Department of Neonatology, Hadassah Hebrew University Medical Center, Jerusalem, Israel

5 Department of Pediatric Surgery, Hadassah Hebrew University Medical Center, Jerusalem, Israel

Introduction

Nanoparticles (NPs) are drawing an increasing interest from many branches of medicine practices and research. Their potential use in medical devices [1] or as drug carriers [2] offers opportunities for novel therapeutic approaches [3] in treating complex disorders such as malignant, inflammatory, and neurodegenerative diseases.

Numerous types of NPs have been designed for systemic and targeted drug delivery. However, keeping NPs in circulating blood for sufficient time to allow them to reach their therapeutic target, is a major challenge. This has become a key challenge due to the fact that the circulation time of NPs is highly limited, since they are quickly cleared from blood stream [4]. Recently, a new strategy for designing a set-up that will provide sufficiently long circulation of NPs has been proposed by Hu et al. [5]. To this end, a class of delivery system has been proposed consisting human red blood cells (RBCs) that interacted with NPs (RBC_{NP}) that are loaded with therapeutic agents [4]. These in vitro-formed RBC_{NP} are injected to the treated subjects [4].

Chambers and Mitragorti [4] demonstrated that polystyrene NPs (PS-NPs) that are usually rapidly cleared from the circulation, can escape clearance when attached to RBC.

Numerous studies have examined NP–RBC interaction, focusing on the penetration of NPs into cells, [6, 7] and the

hemolytic potential of NPs [8–10], while only a few studies investigated the effect of NPs on cell–cell interaction [11, 12]. In these studies, the effects of the size and surface charge of the hydroxyapatite NPs on the RBCs morphology and aggregation were investigated, showing that in protein-free medium, where no aggregation occurs, NPs induced RBC aggregation [11]. The NPs-induced RBC aggregation was lower with negatively charged NPs [11]. Similarly, Simundic et al. reported on the induction of RBC aggregation by TiO_2 and ZnO NPs [12]. In addition, Smyth et al., have shown the induction of platelets aggregation by PS-NPs [13].

To the best of our knowledge, the potential effects of NPs-attached RBC (RBC_{NP}) on the aggregation of untreated RBC and their adherence to vascular endothelial cells (EC) have not been studied.

Previously [10], we studied the hemolytic activity of nanoparticles, using plain polystyrene nanoparticles (PS-NPs), which are well characterized [14–16], and widely used as a reference NP for in vivo [17, 18] and in vitro [16, 19, 20] studies. We have found that PS-NPs, while adhering to RBC [14, 15], exhibit low hemolytic activity (less than 4 %) in protein-free medium [10]. On these grounds, in the present study, we have used these NPs to explore their effects on the aggregation of RBCs and their adherence to vascular EC.

Materials and Methods

Dulbecco's modified Eagle medium (DMEM), fetal calf serum (FCS), penicillin, streptomycin, glutamine, and trypsin were purchased from Biological Industries Ltd, Israel. Poly-L-lysine cell culture glass slides were purchased from Sigma (St. Louis, MO). Polystyrene slides were purchased from Electron Microscopy Science (Washington, PA).

Polystyrene Nanobeads (PS-NPs)

Monodispersed polystyrene (untreated) nanobeads (NIST Traceable Particle Size Standard, 1.0 % solids w/v in an aqueous suspension), purchased from Polysciences, Inc. (Warrington, PA), were 49.9 ± 6.3; 107.9 ± 1.4; 243 ± 3.0 nm in diameter, as determined by the manufacturer, using single particle optical sensing instruments. Previous studies have reported that PS-NPs used here are hydrophobic [21, 22] and have a spherical shape [13, 21].

Preparation of RBC Samples

Permission for the experiment was obtained from the institutional board for human research (Helsinki Committee of the Hadassah Hebrew University Center of Jerusalem, Jerusalem, Israel). Human blood samples were collected from healthy donors. RBCs were isolated from blood by centrifugation, washed (three times) from their plasma by centrifugation (2500 RPM × 5.0 min) in phosphate buffered saline (PBS, pH 7.4), and re-suspended at hematocrit of 10 % in PBS.

Treatment of RBC with NP Suspension

RBC suspension (10 % of cells in PBS buffer) was supplemented with NPs, and incubated for 1 h at 37 °C in a shaking bath (oscillation rate 120 RPM). Particles were added to RBC suspension at concentration from 0.05 up to 0.5 mg/ml. The RBCs were then separated and washed once with PBS by centrifugation (2500 RPM × 5.0 min) and re-suspended at 10 % hematocrit in PBS. The same procedure was applied to control (NPs-free) RBCs.

Supplementation of RBC Suspension with RBC_{NP}

Particle attachment to RBCs was performed according to procedures described above (NP concentration of 0.5 mg/ml). RBC–particle (RBC_{NP}) complexes and untreated RBC are mixed in a ratio of 1/100; 1/50; 1/25; and 1/10 and re-suspended in PBS (10 %).

Endothelial Cell Culture

Transformed human bone marrow endothelial cells (HBMEC) were grown at 37 °C in 5 % CO_2 and 95 % humidity in DMEM supplemented with 10 % FCS, 25 mM Hepes, 100 U/ml penicillin, 100 μg/ml streptomycin, and 2 mM glutamine. The cell cultures were expanded by trypsinization with 0.25 % trypsin in PBS containing 0.025 % EDTA. HBMEC were seeded onto poly-L-lysine glass cell culture slides coated with gelatin (1 %) and grown to confluence.

Measurements of RBC Aggregation

All aggregation measurements were conducted within 6 h of venipuncture. RBC aggregability was studied using a cell flow properties analyzer (CFA) as previously described [23–29].

Briefly, suspension in PBS (6 % hematocrit) of the untreated (control) RBC or RBC_{NP} or their mixture (RBC/RBC_{NP}, in a ratio 100/1; 50/1; 20/1 and 10/1) is introduced into a narrow-gap (30 μm) flow chamber, which is connected to a pump exerting laminar flow and a pressure transducer that monitors shear stress during the experiment. After 10 min of incubation, RBC dynamic organization (aggregation/disaggregation) in the flow chamber is directly visualized and recorded through a microscope

connected to a video camera (TM6EX, Pulnix, USA), which transmits the RBC images to a frame grabber (FlashBus, Integral Technologies Inc, USA) in the computer. Images are then analyzed by original image analysis software to provide parameters of RBC aggregation.

We used three parameters to quantify the degree of cell aggregation, namely, the percent of cells in small aggregations (SAF-small aggregates fraction), large aggregates fraction (LAF) as well as the average aggregate size (AAS) as previously described [25, 30].

Average Aggregate Size (AAS)

We defined the AAS at $\tau = 0.015$ Pa as the peak aggregate size.

Large Aggregate Fraction (LAF)

We measured the distribution of the RBC population into aggregate size ranges, i.e., the erythrocyte fraction (in %) in large aggregates (33 or more RBC per aggregate), for details see [23, 25, 26].

Aggregate Strength Index (ASI)

To obtain an appropriate measure of RBC aggregation, we plotted the AAS as a function of $1/\tau$, and took the slope of this line as an aggregate strength index [31].

Percent of RBC that are Formed (Incorporated) into Aggregates (Ag-RBC, %)

From distribution of RBCs into aggregate size range, we calculated the percent of cells that formed aggregates (size of object is more than one cell).

Determination of RBC/EC Adherence

RBC_{NP}/EC adherence was determined in the cell flow properties analyzer (CFA), as previously described [32]. In brief: the CFA consists of an adaptable narrow-gap flow chamber (0.2 mm) that contains a slide coated with HBMEC. The chamber is placed under a microscope, and connected to a digital camera. The number of adherent RBC was continuously monitored by direct visualization of the cells in the flow chamber, under controllable, increasing shear stress (0.01–3.0 Pa), and their digitized images were transmitted to a computer for analysis and determination of the number of adherent RBCs.

RBC or RBC_{NP} (suspended in Ca^{+2}-PBS, Ca^{+2} concentration is 1.0 mM) were injected into the flow chamber and incubated at 37 °C for 20 min. The RBCs were then washed with the Ca^{+2}-PBS under controllable, increasing flow-induced shear stress, from 0.01–3.0 Pa, and the remaining adherent RBCs were determined as a function of shear stress by the image analysis program. The number of adherent RBCs was continuously counted from images using original software, at each shear stress on 10 randomly chosen fields (with area 0.1 mm^2). The number of adherent RBCs remaining was plotted as a function of $1/\tau$, respective with the equation $N = N_\infty + \alpha/\tau$, where N is the number of adherent RBCs at a specific τ (N_∞ is the number of adherent RBCs at extrapolated $\tau \to \infty$), and α is the adherence coefficient, expressing the strength of intercellular interaction [33, 34].

Statistical Analysis

Data were presented as mean ± SD and tested for statistical significance using the paired Student's t test. P values were considered significant at $p < 0.05$.

Results

We have found that RBC_{NP} (produced by treatment of RBCs with PS-NP) are strong inducers of RBCs self-aggregability (Figs. 1 and 2) and RBCs adherence to EC (Fig. 3). Moreover, these effects were positively correlated with NP concentration.

The treatment of RBCs with PS-NPs caused a formation of RBCs aggregates in protein-free PBS buffer (Fig. 1a). It is known [24, 35], and further illustrated by Fig. 1, that untreated RBC do not form aggregates in a macromolecule-free medium. As shown in Fig. 1b, and in Table 1, both the large aggregate fraction in the RBC population (Fig. 1b) and the AAS (Table 1) grow with increasing PS-NP concentration.

Typical images of adherent RBCs (under 0.1 Pa) are presented in Fig. 2a, and the respective number of adherent RBC are depicted in Fig. 2b and c. These figures clearly show that RBC/EC adhesion is strongly enhanced when RBC are pre-treated with increasing NPs concentration.

An important parameter of RBC/EC adherence is the strength of the intercellular interaction [32–34]. To derive a comprehensive expression of RBC/EC adherence, the values depicted in Fig. 2b, describing the number of adherent RBC as a function of τ, were plotted vs. $1/\tau$, as shown in Fig. 2c. This presentation yields the linear equation, $N = N_\infty + \alpha/\tau$, where N is the number of adherent RBCs at a specific τ, N_∞ is the number of adherent RBCs at infinite shear stress ($\tau \to \infty$), defined as "undetachable" RBC, and α is the adherence coefficient, expressing the strength of intercellular interaction [33, 34].

For determining the appropriate PS-NPs concentration for inducing RBC adhesion to EC, we analyzed the

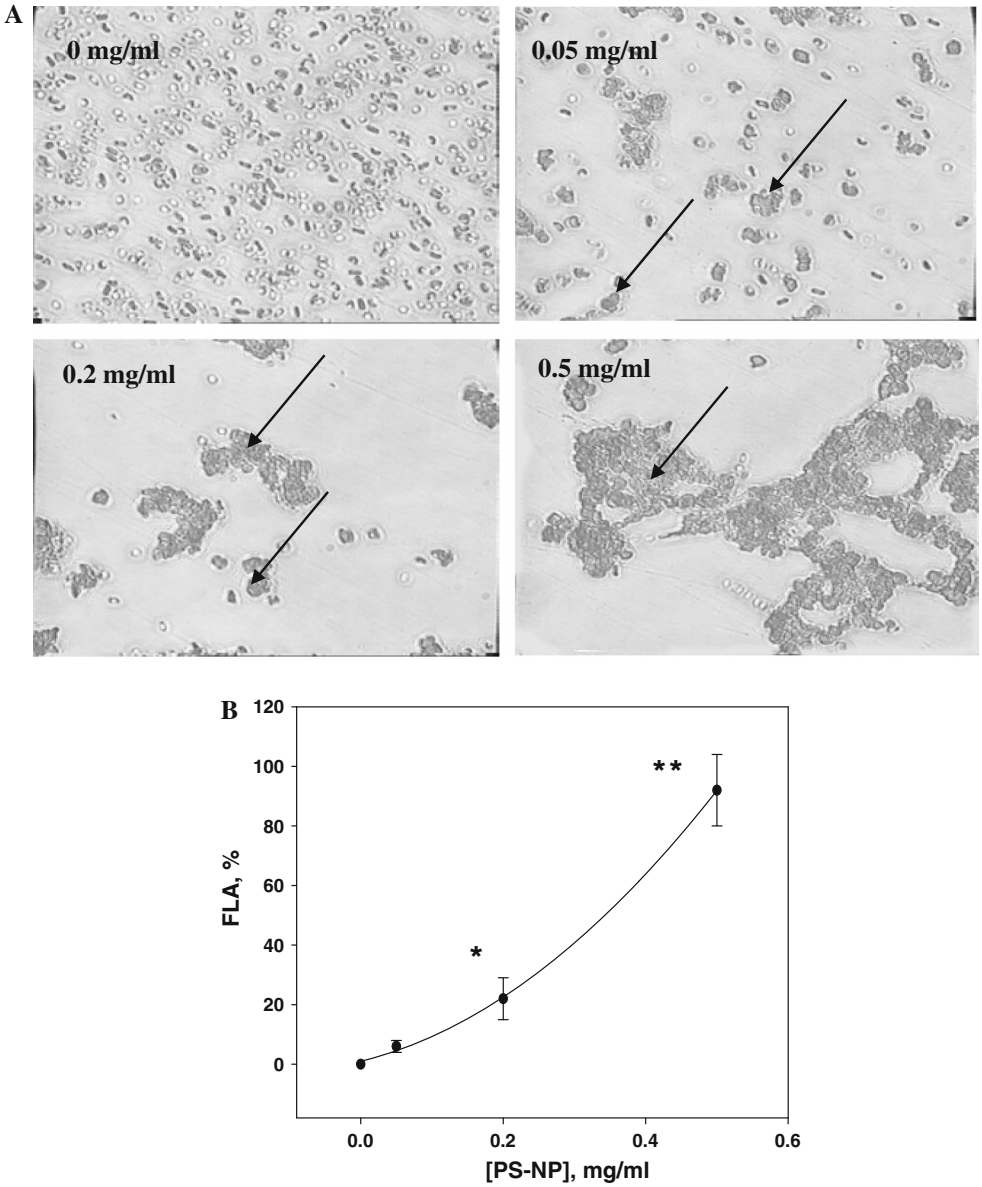

Fig. 1 Aggregation of RBC_{NP}. Treatment of RBC by PS-NPs induced RBC aggregation, in protein-free medium, in concentration dependent manner. **a** Typical images of RBCs, and RBC aggregates in the presence of PS-NPs (marked by *arrows*), at various PS-NP concentrations. **b** RBC fraction in large aggregates (FLA, 33 or more RBC/aggregate) at shear stress of 0.05 Pa. Each datum is mean ± SD for 7 blood samples. Significant difference from non-treated RBC by paired *t* test; $*p < 0.005$, $**p < 0.0001$

dependence of α and N_∞ on NPs concentration. Figure 2c and the derived α and N_∞ values presented in Table 2, show that both the strength of RBC/EC interaction (α), and the number of undetachable RBC, strongly increase with increasing NP concentration.

In addition to testing the effect of NP concentration, we have examined the effect of the NP size, at equal concentration, on RBC intercellular interaction. Unlike the positive correlation with the NP concentration, RBCs aggregation and adherence to EC were inversely correlated with the NP size, as shown in Fig. 3.

As noted in the Introduction, a special interest in the present study was to explore the effects of NPs-attached to RBC (RBC_{NP}) on the aggregation of untreated RBCs and their adherence to vascular EC. To this end, untreated RBCs were mixed with RBCs that had been interacted with PS-NP (RBC_{NP}), as described in Methods, and subjected to determination of aggregation and adherence. As shown in Table 3 (Middle Column) this procedure led to the incorporation of untreated RBC to RBC_{NP} aggregates, as expressed by the increased relative fraction of aggregated RBC in the total RBC population. For example, when only RBC_{NP} were tested the percent of aggregated RBC was 96.5. Accordingly, if only RBC_{NP} form aggregates when the RBC_{NP}/RBC ratio was 1/10, the percent of aggregated RBC should have been about 9.6. However, the aggregation in this case was markedly higher (36.6), implying that these aggregates contain untreated RBC as well.

Following the same logic, Table 3 (Right Column) shows that RBC_{NP} do not induce adhesion of untreated

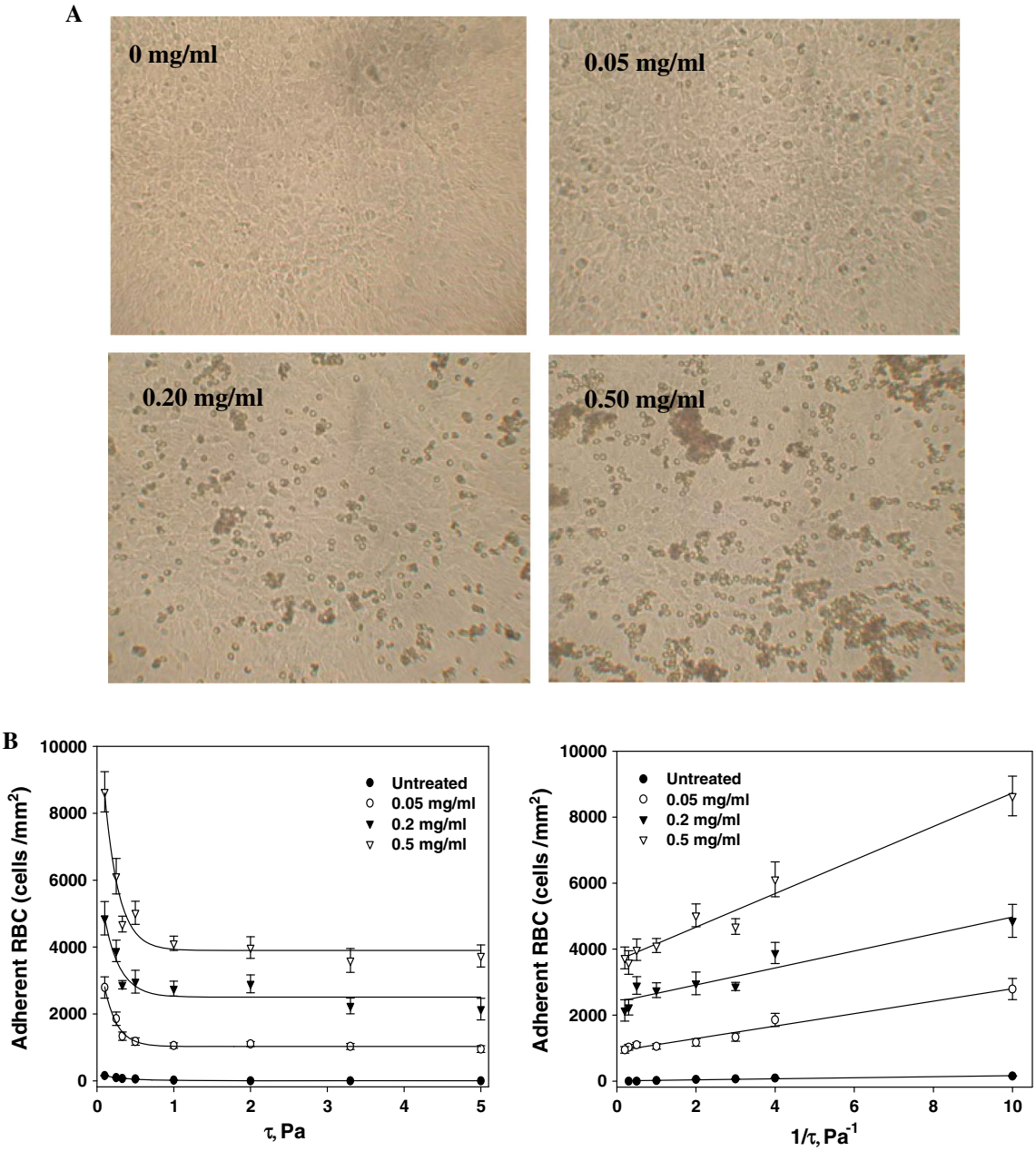

Fig. 2 Treatment of RBC by PS-NPs induced elevation of cells adhesion to EC in concentration dependent manner. **a** Typical adhesion images of RBC (treated and untreated) to EC. Adherence of RBC as a function of τ (**b**) and $1/\tau$ (**c**). The number of adherent RBCs is plotted vs. shear stress (τ). Each datum is mean ± SD for 7 blood samples

RBC, as the number of adherent RBC is proportional to the ratio of RBC_{NP} in the total RBC population.

Discussion

It is well known that NPs interact with biological cells, particularly RBC [8–10] and EC [36]. NPs interact with cells in a different manner than do small molecules, and are taken into the cell by active, energy-dependent processes [36, 37]. There is currently a considerable debate as to the NP characteristics that are important in determining biological response to NP, including their size, shape, and surface area [38]. This interaction, consistent with NP/RBC contact, causes the destruction and hemolysis of RBC [39–41].

In a previous [10] and present study, we used PS-NP, as polystyrene does not generate reactive oxygen species (ROS) in the presence of cells [42], and membrane damage by oxidative stress is unlikely. In addition, the properties of

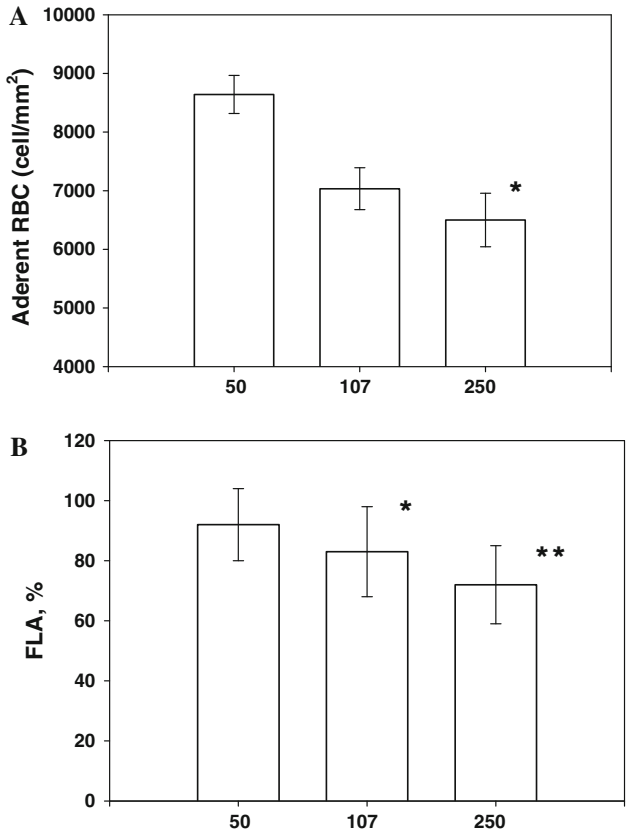

Fig. 3 Initiation of cell–cell interaction by PS-NPs in protein-free medium: Effect of NP size. **a** Initiation of RBCs aggregation (0.05 Pa). **b** Enhancement of RBCs adhesion to EC (0.5 Pa). Concentration of the NP is 0. 50 mg/ml. Each datum is the mean ± SD for 6 RBC samples, obtained from 6 different donors. Significant difference from NP of 50 nm: paired *t* test $*p < 0.05$ and $**p < 0.01$

these NPs are characterized in detail [13–16, 21], and their behavior in various biological systems is well-studied [16, 20, 21, 37, 43–47].

The key finding of the present study is the fact that the treatment of RBCs with PS-NPs initiates a strong cell–cell interaction in protein-free medium, as expressed by the RBCs aggregation and adherence to EC. Han et al. [11] discussed the mechanism of RBC aggregation that was modulated by hydroxyapatite NP, and concluded that NP-induced RBCs aggregation could be attributed to the bridging force via the surfaces of NP and RBCs. The authors consider two alternative models of aggregation of RBCs that have been proposed to describe RBCs aggregation in a medium containing macromolecules, and prefer the bridging model for NPs-induced RBC aggregation [11].

The adhesion of PS-NPs to cells, as shown in previous studies [4, 14, 15, 45], can be attributed to electrostatic and hydrophobic interactions [48–50]. As such, it is plausible that in the case of RBC/RBC and RBC/EC interaction, the PS-NPs bridge between cells, leading to the formation of very large and strong aggregates, and enhanced RBC/EC adhesion.

The extent of RBCs aggregation in a protein-supplemented medium is determined by the balance between opposing forces: the repulsive force between the negatively charged cells, RBC–RBC adhesion induced by the presence of plasma proteins or other macromolecules, and the disaggregating shear force generated by blood flow [51]. Normally, the blood flow is sufficient for dispersion of the RBCs aggregates (in plasma) under shear stress higher than 0.05–0.1 Pa [52]. In contrast, RBC_{NP} aggregates are large (Fig. 2) and are not dispersed by higher-than-normal shear stress (up to 0.4 Pa at high concentration of NPs), as depicted in Table 1.

It is important to underline that the treatment of RBCs with NPs induced strong aggregation in macromolecule-free medium, in which RBCs aggregation does not occur [24, 35].

As in the case of aggregation, we observed a similar phenomenon for the interaction between RBC_{NP} and EC. RBC_{NP} have shown a much stronger interaction with EC than untreated RBC (Fig. 2a) and a flow of 1.0 Pa did not induce a significant detachment of RBC_{NP} from EC (Fig. 2b). We assume that this phenomenon, as in the case of aggregation, may be attributed to the NP-mediated bridging between the cells. It should be noted that attachment of PS-NP to EC has been previously demonstrated [20, 37, 47], thereby implying that the RBC/EC adhesion is exerted by NPs bridging between the two cell types.

As discussed in Introduction, RBCs can be loaded with therapeutic agents without compromising their structural

Table 1 Polystyrene nanoparticles are strong initiator of RBC aggregation

[PS-NP], mg/ml	Average aggregate size (RBCs/aggregate), at shear stress 0.015 Pa, Mean ± SD, $n = 7$.	Aggregate strength index (ASI), Mean ± SD, $n = 7$
0	1.05 ± 0.1	N.A.
0.05	4.26 ± 1.35	9.17 ± 4.5
0.20	15.3 ± 4.56	19.0 ± 9.3
0.50	36.6 ± 8.20	24.03 ± 6.3

Table 2 Polystyrene nanoparticles are strong activator of RBC adhesion to EC

[PS-NP], mg/ml	Adhesion coefficient (α), Pa*(RBCs/mm^2)$^{-1}$ Mean ± SD, $n = 7$	Number of "undetachable" RBC (N_∞), RBCs/mm^2 Mean ± SD, $n = 7$	Correlation coefficient, R^2
0	16 ± 1.2	2.3 ± 3	0.925
0.05	189 ± 34	917 ± 15	0.969
0.20	257 ± 46	2403 ± 23	0.893
0.50	507 ± 32	3655 ± 230	0.969

Table 3 Supplementation of untreated RBCs with RBC_{NP} induced the formation of combined RBC-RBC_{NP} aggregation

RBC_{NP}/RBC ratio	Ag-RBCs[a], % Mean ± SD, $n = 7$	Number of adherent cells (shear stress 0.1 Pa), RBCs/mm^2, Mean ± SD, $n = 7$
RBC only	0	165 ± 19
1/100	3.0 ± 0.7	230 ± 37
1/50	6.2 ± 1.3	320 ± 43
1/25	12.3 ± 4.5	624 ± 73
1/10	36.6 ± 8.2	919 ± 195
RBC_{NP} only	96.5 ± 2.1	8730 ± 1507

[a] Percent of RBCs that incorporated in aggregates (shear stress 0.015 Pa)

integrity and biological functions [53]. Numerous techniques have been proposed for loading NPs with drugs and subsequent attachment to RBC surface [5]. These RBC-based delivery vehicles, classified as 'carrier RBCs,' have been developed for the delivery of numerous therapeutic agents including proteins, nucleic acids, and small-molecule drugs. However, the present study, showing that RBC_{NP} adhere to vascular EC, form self-aggregates, and further facilitates RBC aggregation, demonstrates that the administration of RBC_{NP} can cause deleterious effects in vivo.

Study Limitation

As noted above, in the present study RBCs aggregation and adherence to EC were studied in protein-free medium, while plasma proteins can modulate the properties of NPs, and subsequently their interaction with cells [54–56]. Thus, the extrapolation from the conditions tested in the present study to in vivo conditions needs to be validated.

Conclusion

The present study demonstrates that RBC_{NP} can induce undesired effects on the functionality of RBC and EC in the vascular system, and may respectively induce circulatory disorders. In addition, their cell–cell interactions, may hinder their delivery to the desired target organ. These potential drawbacks should be taken into account when considering the use of RBC_{NP} a drug delivery platform.

Acknowledgments The authors thank Mrs. O. Fredman for technical assistance.

References

1. Holzinger, M., Le Goff, A., & Cosnier, S. (2014). Nanomaterials for biosensing applications: A review. *Frontiers in chemistry, 2*, 63.
2. Rostami, E., Kashanian, S., Azandaryani, A. H., Faramarzi, H., Dolatabadi, J. E., & Omidfar, K. (2014). Drug targeting using solid lipid nanoparticles. *Chemistry and Physics of Lipids, 181*, 56–61.
3. Shvartsman, L., & Laikhtman, B. (2010). Medical application-oriented nanostructure design: Physical basics and limitations. *SPIE Proceedings, 7563*, A1–A10.
4. Chambers, E., & Mitragotri, S. (2004). Prolonged circulation of large polymeric nanoparticles by non-covalent adsorption on erythrocytes. *Journal of Controlled Release, 100*, 111–119.
5. Hu, C. M., Fang, R. H., & Zhan, L. (2013). Erythrocyte-inspired delivery systems. *Advanced Healthcare Materials, 1*, 537–547.
6. Gutierrez Millan, C., Colino Gandarillas, C. I., Sayalero Marinero, M. L., & Lanao, J. M. (2012). Cell-based drug-delivery platforms. *Therapeutic Delivery, 2012*(3), 25–41.
7. Wang, T., Bai, J., Jiang, X., & Nienhaus, G. U. (2012). Cellular uptake of nanoparticles by membrane penetration: a study combining confocal microscopy with FTIR spectroelectrochemistry. *ACS Nano, 6*, 1251–1259.
8. Choi, J., Reipa, V., Hitchins, V. M., Goering, P. L., & Malinauskas, R. A. (2012). Physicochemical characterization and

in vitro hemolysis evaluation of silver nanoparticles. *Toxicological Sciences, 123*, 133–143.
9. Yu, T., Malugin, A., & Ghandehari, H. (2012). Impact of silica nanoparticle design on cellular toxicity and hemolytic activity. *ACS Nano, 5*, 5717–5728.
10. Barshtein, G., Arbell, D., & Yedgar, S. (2011). Hemolytic effect of polymeric nanoparticles: role of albumin. *IEEE Transactions on Nanobioscience, 10*, 259–261.
11. Han, Y., Wang, X., Dai, H., & Li, S. (2012). Nanosize and surface charge effects of hydroxyapatite nanoparticles on red blood cell suspensions. *ACS Applied Materials & Interfaces, 4*, 4616–4622.
12. Simundic, M., Drasler, B., Sustar, V., Zupanc, J., Stukelj, R., Makovec, D., et al. (2013). Effect of engineered TiO2 and ZnO nanoparticles on erythrocytes, platelet-rich plasma and giant unilamelar phospholipid vesicles. *BMC Veterinary Research, 9*, 7.
13. Smyth, E., Solomon, A., Vydyanath, A., Luther, P. K., Pitchford, S., Tetley, T. D., & Emerson, M. (2015). Induction and enhancement of platelet aggregation in vitro and in vivo by model polystyrene nanoparticles. *Nanotoxicology, 9*, 356–364.
14. Chambers, E., & Mitragotri, S. (2007). Long circulating nanoparticles via adhesion on red blood cells: mechanism and extended circulation. *Experimental Biology and Medicine (Maywood), 232*, 958–966.
15. Zook, J. M., Maccuspie, R. I., Locascio, L. E., Halter, M. D., & Elliott, J. T. (2011). Stable nanoparticle aggregates/agglomerates of different sizes and the effect of their size on hemolytic cytotoxicity. *Nanotoxicology, 5*, 517–530.
16. Brown, D. M., Wilson, M. R., MacNee, W., Stone, V., & Donaldson, K. (2001). Size-dependent proinflammatory effects of ultrafine polystyrene particles: a role for surface area and oxidative stress in the enhanced activity of ultrafines. *Toxicology and Applied Pharmacology, 175*, 191–199.
17. Geiser, M., Rothen-Rutishauser, B., Kapp, N., Schurch, S., Kreyling, W., Schulz, H., et al. (2005). Ultrafine particles cross cellular membranes by nonphagocytic mechanisms in lungs and in cultured cells. *Environmental Health Perspectives, 113*, 1555–1560.
18. Papageorgiou, I., Brown, C., Schins, R., Singh, S., Newson, R., Davis, S., et al. (2007). The effect of nano- and micron-sized particles of cobalt-chromium alloy on human fibroblasts in vitro. *Biomaterials, 28*, 2946–2958.
19. Kato, T., Yashiro, T., Murata, Y., Herbert, D. C., Oshikawa, K., Bando, M., et al. (2003). Evidence that exogenous substances can be phagocytized by alveolar epithelial cells and transported into blood capillaries. *Cell and Tissue Research, 311*, 47–51.
20. Yacobi, N. R., Demaio, L., Xie, J., Hamm-Alvarez, S. F., Borok, Z., Kim, K. J., & Crandall, E. D. (2008). Polystyrene nanoparticle trafficking across alveolar epithelium. *Nanomedicine, 4*, 139–145.
21. McGuinnes, C., Duffin, R., Brown, S., Mill, N., Megson, I. L., Macnee, W., et al. (2011). Surface derivatization state of polystyrene latex nanoparticles determines both their potency and their mechanism of causing human platelet aggregation in vitro. *Toxicological Sciences, 119*, 359–368.
22. Mielczarski, J. A., Jeyachandran, Y. L., Mielczarski, E., & Rai, B. (2011). Modification of polystyrene surface in aqueous solutions. *Journal of Colloid and Interface Science, 362*, 532–539.
23. Ami, R. B., Barshtein, G., Zeltser, D., Goldberg, Y., Shapira, I., Roth, A., et al. (2001). Parameters of red blood cell aggregation as correlates of the inflammatory state. *American Journal of Physiology Heart and Circulatory Physiology, 280*, H1982–H1988.
24. Barshtein, G., Wajnblum, D., & Yedgar, S. (2000). Kinetics of linear rouleaux formation studied by visual monitoring of red cell dynamic organization. *Biophysical Journal, 78*, 2470–2474.
25. Ben-Ami, R., Barshtein, G., Mardi, T., Deutch, V., Elkayam, O., Yedgar, S., & Berliner, S. (2003). A synergistic effect of albumin and fibrinogen on immunoglobulin-induced red blood cell aggregation. *American Journal of Physiology Heart and Circulatory Physiology, 285*, H2663–H2669.
26. Ben-Ami, R., Sheinman, G., Yedgar, S., Eldor, A., Roth, A., Berliner, A. S., & Barshtein, G. (2002). Thrombolytic therapy reduces red blood cell aggregation in plasma without affecting intrinsic aggregability. *Thrombosis Research, 105*, 487–492.
27. Berliner, S., Ben-Ami, R., Samocha-Bonet, D., Abu-Abeid, S., Schechner, V., Beigel, Y., et al. (2004). The degree of red blood cell aggregation on peripheral blood glass slides corresponds to inter-erythrocyte cohesive forces in laminar flow. *Thrombosis Research, 114*, 37–44.
28. Chen, S., Gavish, B., Barshtein, G., Mahler, Y., & Yedgar, S. (1994). Red blood cell aggregability is enhanced by physiological levels of hydrostatic pressure. *Biochimica et Biophysica Acta, 1192*, 247–252.
29. Chen, S., Eldor, A., Barshtein, G., Zhang, S., Goldfarb, A., Rachmilewitz, E., & Yedgar, S. (1996). Enhanced aggregability of red blood cells of beta-thalassemia major patients. *The American Journal of Physiology, 270*, H1951–H1956.
30. Chen, S., Gavish, B., Zhang, S., Mahler, Y., & Yedgar, S. (1995). Monitoring of erythrocyte aggregate morphology under flow by computerized image analysis. *Biorheology, 32*, 487–496.
31. Barshtein, G., Ponizovsky, A. M., Nechamkin, Y., Ritsner, M., Yedgar, S., & Bergelson, L. D. (2004). Aggregability of red blood cells of schizophrenia patients with negative syndrome is selectively enhanced. *Schizophrenia Bulletin, 30*, 913–922.
32. Ramot, Y., Koshkaryev, A., Goldfarb, A., Yedgar, S., & Barshtein, G. (2008). Phenylhydrazine as a partial model for beta-thalassaemia red blood cell hemodynamic properties. *British Journal of Haematology, 140*, 692–700.
33. Koshkaryev, A., Barshtein, G., Nyska, A., Ezov, N., Levin-Harrus, T., Shabat, S., et al. (2003). 2-Butoxyethanol enhances the adherence of red blood cells. *Archives of Toxicology, 77*, 465–469.
34. Koshkaryev, A., Barshtein, G., & Yedgar, S. (2010). Vitamin E induces phosphatidylserine externalization and red cell adhesion to endothelial cells. *Cell Biochemistry and Biophysics, 56*, 109–114.
35. Barshtein, G., Tamir, I., & Yedgar, S. (1998). Red blood cell rouleaux formation in dextran solution: dependence on polymer conformation. *European Biophysics Journal : EBJ., 27*, 177–181.
36. Peetla, C., & Labhasetwar, V. (2008). Biophysical characterization of nanoparticle-endothelial model cell membrane interactions. *Molecular Pharmaceutics, 5*, 418–429.
37. Guarnieri, D., Guaccio, A., Fusco, S., & Netti, P. A. (2011). Effect of serum proteins on polystyrene nanoparticle uptake and intracellular trafficking in endothelial cells. *Journal of Nanoparticle Research, 13*, 4295–4309.
38. Nel, A., Xia, T., Madler, L., & Li, N. (2006). Toxic potential of materials at the nanolevel. *Science, 311*, 622–627.
39. Dash, B. C., Rethore, G., Monaghan, M., Fitzgerald, K., Gallagher, W., & Pandit, A. (2010). The influence of size and charge of chitosan/polyglutamic acid hollow spheres on cellular internalization, viability and blood compatibility. *Biomaterials, 31*, 8188–8197.
40. Lin, Y. S., & Haynes, C. L. (2010). Impacts of mesoporous silica nanoparticle size, pore ordering, and pore integrity on hemolytic activity. *Journal of the American Chemical Society, 132*, 4834–4842.
41. Dobrovolskaia, M. A., Clogston, J. D., Neun, B. W., Hall, J. B., Patri, A. K., & McNeil, S. E. (2008). Method for analysis of nanoparticle hemolytic properties in vitro. *Nano Letters, 8*, 2180–2187.

42. Wang, M. L., Hauschka, P. V., Tuan, R. S., & Steinbeck, M. J. (2002). Exposure to particles stimulates superoxide production by human THP-1 macrophages and avian HD-11EM osteoclasts activated by tumor necrosis factor-alpha and PMA. *Journal of Arthroplasty, 17*, 335–346.
43. Blank, F., Rothen-Rutishauser, B., & Gehr, P. (2007). Dendritic cells and macrophages form a transepithelial network against foreign particulate antigens. *American Journal of Respiratory Cell and Molecular Biology, 36*, 669–677.
44. Mrakovcic, M., Absenger, M., Riedl, R., Smole, C., Roblegg, E., Frohlich, L. F., & Frohlich, E. (2013). Assessment of long-term effects of nanoparticles in a microcarrier cell culture system. *PLoS One, 8*, e56791.
45. Rothen-Rutishauser, B. M., Schurch, S., Haenni, B., Kapp, N., & Gehr, P. (2006). Interaction of fine particles and nanoparticles with red blood cells visualized with advanced microscopic techniques. *Environmental Science and Technology, 40*, 4353–4359.
46. Jiang, X. E., Dausend, J., Hafner, M., Musyanovych, A., Rocker, C., Landfester, K., et al. (2010). Specific effects of surface amines on polystyrene nanoparticles in their interactions with mesenchymal stem cells. *Biomacromolecules, 11*, 748–753.
47. Yacobi, N. R., Malmstadt, N., Fazlollahi, F., DeMaio, L., Marchelletta, R., Hamm-Alvarez, S. F., et al. (2010). Mechanisms of alveolar epithelial translocation of a defined population of nanoparticles. *American Journal of Respiratory Cell and Molecular Biology, 42*, 604–614.
48. Yoon, J. Y., Kim, J. H., & Kim, W. S. (1998). Interpretation of protein adsorption phenomena onto functional microspheres. *Colloid Surface B, 12*, 15–22.
49. Yoon, J. Y., Park, H. Y., Kim, J. H., & Kim, W. S. (1996). Adsorption of BSA on highly carboxylated microspheres—Quantitative effects of surface functional groups and interaction forces. *Journal of Colloid and Interface Science, 177*, 613–620.
50. Anselmo, A. C., Gupta, V., Zern, B. J., Pan, D., Zakrewsky, M., Muzykantov, V., & Mitragotri, S. (2013). Delivering Nanoparticles to Lungs while Avoiding Liver and Spleen through Adsorption on Red Blood Cells. *ACS Nano, 7*, 11129–11137.
51. Chien, S., & Jan, K. (1973). Ultrastructural basis of the mechanism of rouleaux formation. *Microvascular Research, 5*, 155–166.
52. Barshtein, G., Ben-Ami, R., & Yedgar, S. (2007). Role of red blood cell flow behavior in hemodynamics and hemostasis. *Expert Review of Cardiovascular Therapy, 5*, 743–752.
53. Ihler, G. M., Glew, R. H., & Schnure, F. W. (1973). Enzyme loading of erythrocytes. *Proceedings of the National Academy of Sciences, 70*, 2663–2666.
54. Casals, E., Pfaller, T., Duschl, A., Oostingh, G. J., & Puntes, V. (2010). Time evolution of the nanoparticle protein corona. *ACS Nano, 4*, 3623–3632.
55. Cedervall, T., Lynch, I., Lindman, S., Berggard, T., Thulin, E., Nilsson, H., et al. (2007). Understanding the nanoparticle-protein corona using methods to quantify exchange rates and affinities of proteins for nanoparticles. *Proceedings of the National Academy of Sciences, 104*, 2050–2055.
56. Treuel, L., Docter, D., Maskos, M., & Stauber, R. H. (2015). Protein corona—from molecular adsorption to physiological complexity. *Beilstein Journal of Nanotechnology, 6*, 857–873.